Cellulose (2014) 21:335–346
DOI 10.1007/s10570-013-0158-2

ORIGINAL PAPER

Preparation and characterization of nanocrystalline cellulose via low-intensity ultrasonic-assisted sulfuric acid hydrolysis

Yanjun Tang · Shujie Yang · Nan Zhang · Junhua Zhang

Received: 1 July 2013 / Accepted: 21 December 2013 / Published online: 29 December 2013

Abstract Nanocrystalline cellulose (NCC) was extracted from microcrystalline cellulose via low-intensity ultrasonic-assisted sulfuric acid hydrolysis process. NCC samples were characterized by scanning electron microscopy (SEM), transmission electron microscopy (TEM), particle size distribution (PSD) analysis, Fourier-transformed infrared spectra (FT-IR), X-ray diffraction (XRD), thermogravimetric analysis (TGA) and rheological measurement. It was found that NCC yield reached 40.4 % under the optimum process of low-intensity ultrasonic-assisted sulfuric acid hydrolysis, while it was only 33.0 % in the absence of ultrasonic treatment. Furthermore, the results showed that the two NCC samples obtained from ultrasonic-assisted hydrolysis and conventional hydrolysis were very similar in morphology, both exhibiting rod-like structures with widths and lengths of 10–20 and 50–150 nm, respectively. XRD result revealed that the NCC sample from ultrasonic-assisted hydrolysis contained a small amount of cellulose II and possessed a Segal Crystallinity Index of 90.38 % and a crystallite size of 58.99 Å, higher than those of the NCC sample from conventional hydrolysis. Moreover, PSD analysis demonstrated that the former exhibited a smaller value in average particle size than the latter. In addition, rheological measurements showed that the NCC suspensions from the ultrasonic-assisted process exhibited a lower viscosity over the range of shear rate from 0.1 to 100 s^{-1} in comparison with that prepared in the absence of ultrasonic treatment.

Keywords Nanocrystalline cellulose · Sulfuric acid hydrolysis · Ultrasonic treatment · Yield · Microstructure

Y. Tang (✉) · S. Yang · J. Zhang
Key Laboratory of Advanced Textile Materials and Manufacturing Technology, Ministry of Education, Zhejiang Sci-Tech University, Hangzhou 310018, China
e-mail: tangyj@zstu.edu.cn

Y. Tang
Limerick Pulp and Paper Center, University of New Brunswick, Fredericton E3B 5A3, Canada

N. Zhang
Shanghai Tonnor Material Science Co., Ltd., Shanghai 200092, China

J. Zhang
Engineering Research Center for Eco-Dyeing & Finishing of Textiles, Ministry of Education, Zhejiang Sci-Tech University, Hangzhou 310018, China

Introduction

Nanocrystalline cellulose (NCC), can be produced from a great variety of sources such as microcrystalline cellulose (MCC) (Liu et al. 2011; Satyamurthy et al. 2011), bacterial cellulose (Roman and Winter 2004), cotton (Morais et al. 2012), hardwood (Eronen et al. 2011) and softwood (de Morais Teixeira et al. 2010).

NCC not only has the inherent characteristics of natural cellulose (Fatehi et al. 2010; Qian et al. 2009), but also exhibits such appealing properties as high crystallinity index (>70 %), large surface area ($\sim$150 m^2/g), big aspect ratio ($\sim$70) and high tensile strength (7,500 MPa) (Lam et al. 2012). Owing to these features, in recent years, NCC has gained increasing attention in various fields including regenerative medicine (Klemm et al. 2001), printing applications (Torvinen et al. 2012), optical application (Okahisa et al. 2011), and composite materials (Zaman et al. 2012a).

Various methods have been adopted for the preparation of NCC. These include steam explosion treatment (Deepa et al. 2011), high pressure homogenization (Li J et al. 2012), ultrasonic technique (Li W et al. 2012), acid-/alkaline-hydrolysis (Johar et al. 2012; Zaman et al. 2012b) and enzyme-assisted hydrolysis (Henriksson et al. 2007), as well as the combined processes (Chen et al. 2011a; Chen et al. 2013; Lu et al. 2013). These methods can be used to produce different types of NCC (Elazzouzi-Hafraoui et al. 2007). Among these methods, acid hydrolysis has been commonly used for NCC extraction because of its moderate operation conditions and the good stability of the resulting suspensions (Beck-Candanedo et al. 2005). However, a number of limitations still need to be reconsidered, such as potential degradation of cellulose, time-consuming production process and low yield (Brinchi et al. 2013). To overcome these drawbacks, some new methods have been developed, such as purely physical method of high-intensity ultrasonication (Tischer et al. 2010), and ultrasonic-assisted chemical method (Chen et al. 2011b; de Campos et al. 2013; Wang et al. 2008). Ultrasound energy can be transferred to cellulose chains through a cavitation process involving the formation, expansion, and implosion of cavities in a liquid (Filson and Dawson-Andoh 2009). As a consequence, the mechanical shearing forces generally break down the interaction force between cellulose microfibrils, facilitating the disintegration of cellulosic fibers into nanofibers.

In recent years, an increasing effort has been devoted to the study regarding the integration of chemical process and high-intensity ultrasonic treatment to produce NCC. Filson and Dawson-Andoh (2009) examined the production of cellulose nanocrystals from MCC, avicel and recycled pulp using high-intensity ultrasonic (1,050 W) assisted acid hydrolysis. Chen et al. (2011b) investigated the individualization of cellulose nanofibers from poplar wood using high-intensity (400–1,200 W) combined with chemical treatment. More recently, Chen et al. (2013) reported the disintegration of NCC through chemical pretreatment and high-intensity ultrasonication (1,200 W), and studied the dynamic rheological behavior of NCC suspensions. However, the ultrasonic effect is non-selective, indicating that it can remove both the amorphous and crystalline cellulose (Li W et al. 2012). The higher the intensity of ultrasonication, the lower the crystallinity of the obtained NCC, and then there would be less significant effect on the potential application in nanocomposites. Actually, ultrasound has been known to be divided into "high" and "low" intensity (Ahmadi et al. 2012). Low-intensity ultrasonication is believed to generate an unfocused ultrasonic beam (Ahmadi et al. 2012; Pourbafarani et al. 2013), which can be assumed to be an effective alternative method to facilitate the acid hydrolysis process of cellulose under a fairly mild cavitation. In the present work, to verify the above assumption, NCC samples were prepared from MCC via sulfuric acid hydrolysis assisted by low-intensity ultrasonication and conventional sulfuric acid hydrolysis. A comparative study on the NCC yield, and the morphological/structural characteristics of NCC prepared in the presence or absence of ultrasonic treatment was carried out. Initially, the effects of sulfuric acid concentration and ultrasonic time on the NCC yield, a key factor determining the economics of the hydrolysis process, were discussed. Then, the morphological and structural characteristics of the NCC samples were studied using scanning electron microscopy (SEM), transmission electron microscopy (TEM), Fourier-transformed infrared spectra (FT-IR), X-ray diffraction (XRD), and thermogravimetric analysis (TGA) techniques. Moreover, the particle size distribution (PSD) analysis and rheological behavior of NCC suspensions were studied.

Experimental

Raw materials

Commercial MCC powder was provided by Shanghai Tonnor Material Science Co., Ltd. (Shanghai, China) and selected as the raw material for the extraction of NCC. Sulfuric acid (H_2SO_4, 95 wt%) and dialysis bags

(MW cut off 10,000) were purchased from Hangzhou Mike Chemical Instrument Co., Ltd. (Hangzhou, China). Distilled water was used for all experiments.

Preparation of NCC

Five grams of MCC were added into 50 mL of sulfuric acid (59, 61, 63, 64, 65, 66 %, 67, wt%) solution in a three-neck round-bottom flask. The hydrolysis was performed at 50 °C under stirring by using an electrical agitator (IKA RW20) for 90 min. The resulted dispersion was treated in a common ultrasonic generator (KQ-200VDE, Kunshan ultrasonic instrument Co., Ltd., China) with a constant power of 100 W to promote the acid hydrolysis. The ultrasonic intensity is 0.22 W/cm^2, which is calculated by dividing power with the bottom area (30 cm × 15 cm) (Liu et al. 2009), so it seems that there is an insignificant occurrence of cavitation bubbles. To investigate the effect of ultrasonic time on NCC yield, the ultrasonic treatment was conducted for 10, 20, 30, 40, and 50 min, respectively. After the ultrasonic-assisted hydrolysis was run for a desired duration, 400 mL of deionized water was added into the flask to terminate the hydrolysis. Subsequently, the resulting mixture was centrifuged at 11,000 rpm for 10 min (TGL-16, Wei Jia Instrument Manufacturing Co., LTD., China) to separate the nanocellulose. Meanwhile, the nanocellulose was washed with deionized water and repeatedly centrifuged for 5 times. The fresh colloidal suspension of nanocellulose was filtered with distilled water in a dialysis bag for 2 days to a constant pH of 7.0. The suspension was collected and freeze-dried for testing. Finally, the NCC sample prepared via low-intensity ultrasonic-assisted sulfuric acid hydrolysis was denoted as NCC-65-30, where 65 is H_2SO_4 concentration (wt%) and 30 stands for the ultrasonic time (min). In order to investigate the effects of the ultrasonic treatment, these procedures were repeated under the same conditions but in the absence of ultrasonic treatment, that is, these samples prepared via a conventional method were named as NCC-65.

Calculation of NCC yield

After dialysis, the total volume of NCC suspension was measured. A specified amount (mL) of the NCC suspension was then quickly transferred to a weighing bottle, and dried at 105 °C to a constant weight. Finally, after cooling down to room temperature, the sample was weighed with an analytical balance. The final result for each sample was obtained as the average of three runs of measurements. The yield (%) was calculated according to Eq. (1):

$$\text{Yield}(\%) = \frac{(m_1 - m_2) \times V_1}{m_3 \times V_2} \times 100 \quad (1)$$

Where m_1 is the total mass of oven-dried NCC and weight bottle (mg), m_2 is the mass of the weight bottle (mg), m_3 is the mass of MCC (mg), V_1 is the total volume of as-prepared NCC suspension (mL), V_2 is the volume of NCC to be oven-dried (mL).

Field emission scanning electron microscopy (FE-SEM)

The morphology of NCC and MCC samples was observed by using a ULTRA-55 field-emission scanning electron microscope (FE-SEM, JEOL, Japan). All samples were coated with gold before observation.

Transmission electron microscopy (TEM)

Initially, NCC sample was ultrasonically dispersed in anhydrous ethanol to form a NCC suspension. Then, small droplet of the diluted NCC suspension was deposited on a 300 mesh copper grid coated with holey carbon film. The excess liquid was removed by filteration. The as-obtained specimen was subsequently dried under an infrared lamp for 5 min. Subsequently, TEM images were obtained by using a JSM-2100 transmission electron microscopy (JEOL, Japan) at an accelerating voltage of 80 kV.

Particle size distribution (PSD) analysis

The PSDs of MCC and NCC samples were determined using Malvern Zetasizer 2000 and Malvern Zetasizer NanoZS90 (Malvern Instruments Ltd., UK), respectively.

Fourier-transformed infrared spectra (FT-IR) analysis

Fourier-transformed infrared spectra of NCC and MCC samples were obtained on Nicolet 5700

spectrometer (Thermo Fisher Scientific, USA) with a resolution of 4 cm^{-1} in the range of 4,000–400 cm^{-1}, for which the samples were pelletized with KBr powder.

X-ray diffraction (XRD) analysis

X-ray diffraction patterns for MCC and NCC samples were performed on a diffractometer (X'TRA-055, ARL, Switzerland) with Cu Kα radiation ($\lambda = 0.154$ nm) at 40 kV and 40 mA. XRD data were collected from $2\theta = 10°$–$40°$ at a scan rate of 2°/min (Qua et al. 2011). The diffraction patterns calculated from cellulose Iβ (Nishiyama et al. 2002) and II (Langan et al. 2001) structures were used to simulate the experimental data of MCC and NCC samples. Various diffraction intensities were output by the Mercury program from the Cambridge Crystallographic Data Centre (CCDC). Based on the Mercury program, the XRD-based Segal Crystallinity Index (CI) for MCC, NCC-65 and NCC-65-30 was calculated by following the procedure recently reported in the literature (French and Santiago Cintrón 2013). Crystal information files (.cif) and structures for cellulose Iβ and II were derived from the Supplementary Material in the most recent literature (French 2014). Moreover, to better understand the crystal structure of various cellulose samples, the crystallite size of MCC and NCC samples was also calculated by Scherrer formula (French and Santiago Cintrón 2013; Scherrer 1918).

Thermogravimetric analysis (TGA)

The thermal behavior of NCC and MCC samples was determined using Pyrisl TGA (PerKin Elmer, USA) under nitrogen atmosphere from room temperature up to 800 °C at a heating rate of 20 °C/min.

Rheological measurements

The rheological behavior of the NCC suspensions was performed on a cylinder rotary rheometer (Physica MCR301, Anton Paar, Austria) at 25 °C. The viscosity was measured over a range of shear rates from 0.1 to 100 s^{-1}.

Results and discussion

Effect of sulfuric acid concentration on NCC yield

Sulfuric acid concentration is one of the most important factors affecting the extraction of NCC during acid hydrolysis. Too high a sulfuric acid concentration can lead to the serious degradation of cellulose to sugars, but too low a sulfuric acid concentration may make fibers poorly dispersed and even aggregated (Fan and Li 2012). There are fairly narrow ranges of sulfuric acid concentrations for different materials. Bondeson et al. (2006) optimized the acid hydrolysis process for production of NCC from MCC. The NCC yield reached 30.0 % when sulfuric acid concentration was set at 63.5 wt%. Hamad and Hu (2010) conducted a systematic investigation of the structure–process–yield interrelations in the NCC extraction from a commercial softwood Kraft pulp. NCC with a high crystallinity (>80 %) and a yield between 21 and 38 % can be obtained using 64 wt% sulfuric acid. In this work, a series of hydrolysis experiments with different sulfuric acid concentrations at 50 °C for 90 min were compared for the enhancement of NCC yield, and the results are shown in Table 1. It is clear that sulfuric acid concentration had a marked effect on NCC yield. When the sulfuric acid concentration increased from 59 to 65 wt%, there was a significant increase in the NCC yield. NCC yield can reach the maximum of 33.0 % based on the sulfuric acid concentration of 65 wt% during hydrolysis. However, an adverse trend can be observed from Table 1 that MCC was fully degraded to produce sugar molecules when further increasing the sulfuric acid concentration to 67 wt%. As a result, too high a sulfuric acid concentration was indeed unfavorable for the

Table 1 Effect of sulfuric acid concentration on the NCC yield

Sulfuric acid concentration (wt%)	Yield (%)
59	15.1 ± 1.1
61	22.8 ± 0.9
63	29.6 ± 1.0
64	31.4 ± 0.5
65	33.0 ± 1.0
66	15.2 ± 0.7
67	–

extraction of NCC, and the optimum concentration was set at 65 wt%, which was used in the subsequent procedures of this work.

Effect of low-intensity ultrasonic time on NCC yield

Based on the sulfuric acid hydrolysis experiments mentioned above, ultrasonic treatment was employed to improve the yield of NCC. Recently, NCC samples from a variety of cellulosic sources have been prepared by using high-intensity ultrasonication combined with acid hydrolysis (Chen et al. 2011c; Tang et al. 2012). However, in the literature, there have been limited studies regarding the enhancement of NCC yield by using ultrasonic treatment. In this work, the effect of low-intensity ultrasonic time on the NCC yield was investigated, and the results are shown in Fig. 1. It can be seen that the yield of NCC derived from sulfuric acid hydrolysis in the absence of ultrasonic treatment was only 33.0 %. Interestingly, with further low-ultrasonic treatment for 20 and 30 min, the resulted NCC had a yield of 35.0 and 40.4 % (see Fig. 1), respectively, which showed a percentage increase of 6.1 and 22.4 %. However, there was no significant increase in NCC yield with further increase of the ultrasonic time from 30 to 50 min. The above results indicated that the ultrasonic treatment had an obvious impact on NCC yield. Actually, this may be explained by the effect of acoustic cavitation. The emission of heat and excited species via the cavitation effect can relax the MCC surface and lead to bond breakages, particularly in the lattice defects of MCC (Cintas and Luche 1999). Thus, the use of ultrasonic treatment can facilitate the interaction between single fiber and micro bubbles generated by the ultrasound equipment, which further disintegrates MCC fibers into NCC. Taking the cost and efficiency into consideration, the optimal ultrasonic time for NCC extraction was chosen to be 30 min.

Morphology and structure characterization

SEM images of the MCC and NCC samples are shown in Fig. 2. It can be seen that MCC particles exhibited curled and well-defined fibrils, with widths in the range of 10–20 μm (Fig. 2a). After sulfuric acid hydrolysis, the MCC was separated into nano-sized cellulose. The width of NCC-65 was about 15–30 nm

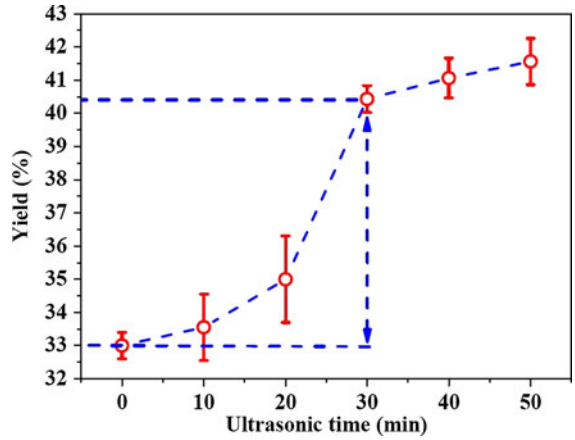

Fig. 1 Effect of ultrasonic time on the NCC yield (Other conditions: sulfuric acid concentration of 65 wt%, temperature of 50 °C, hydrolysis time of 90 min; ultrasonic output power of 100 W)

(Fig. 2b). With further ultrasonic treatment for 30 min, it can be seen more clearly in Fig. 2c that the width and length of the NCC particles were in the range of about 10–20 and 50–150 nm, respectively. Moreover, it was apparent that NCC-65 and NCC-65-30 displayed a regular rod-like structure, similar to that observed in previous studies (Bai et al. 2009; Pirani and Hashaikeh 2012).

Figure 2d–f shows the TEM images of MCC and NCC samples. Aggregates consisting of net-work cellulose fibers with nanoscale widths can be observed in Fig. 2e, f. Similar observations were reported in the literature (Hashaikeh and Abushammala 2011; Lu and Hsieh 2010). Hashaikeh and Abushammala (2011) produced network-structured nanocellulose by sulfuric acid dissolution of MCC and regeneration in ethanol. It was hypothesized that the chains bundled or twisted together randomly and networking occurred when chains were split to join different bundles. Lu et al. (2013) also prepared network structure morphologies with acid hydrolysis of cotton cellulose, and it was found that the strong H-bonding among NCC overcame the repulsion of surface negative charges and led to the formation of self-assembled porous networks. In addition, it can be seen from the TEM images that the net-work diameter gradually became smaller from raw MCC (Fig. 2d), NCC-65 (Fig. 2e) to NCC-65-30 (Fig. 2f), which can be attributed to the effect of acid hydrolysis and acoustic cavitation.

The PSD and average size of MCC, NCC-65, and NCC-65-30 were determined, and the results are

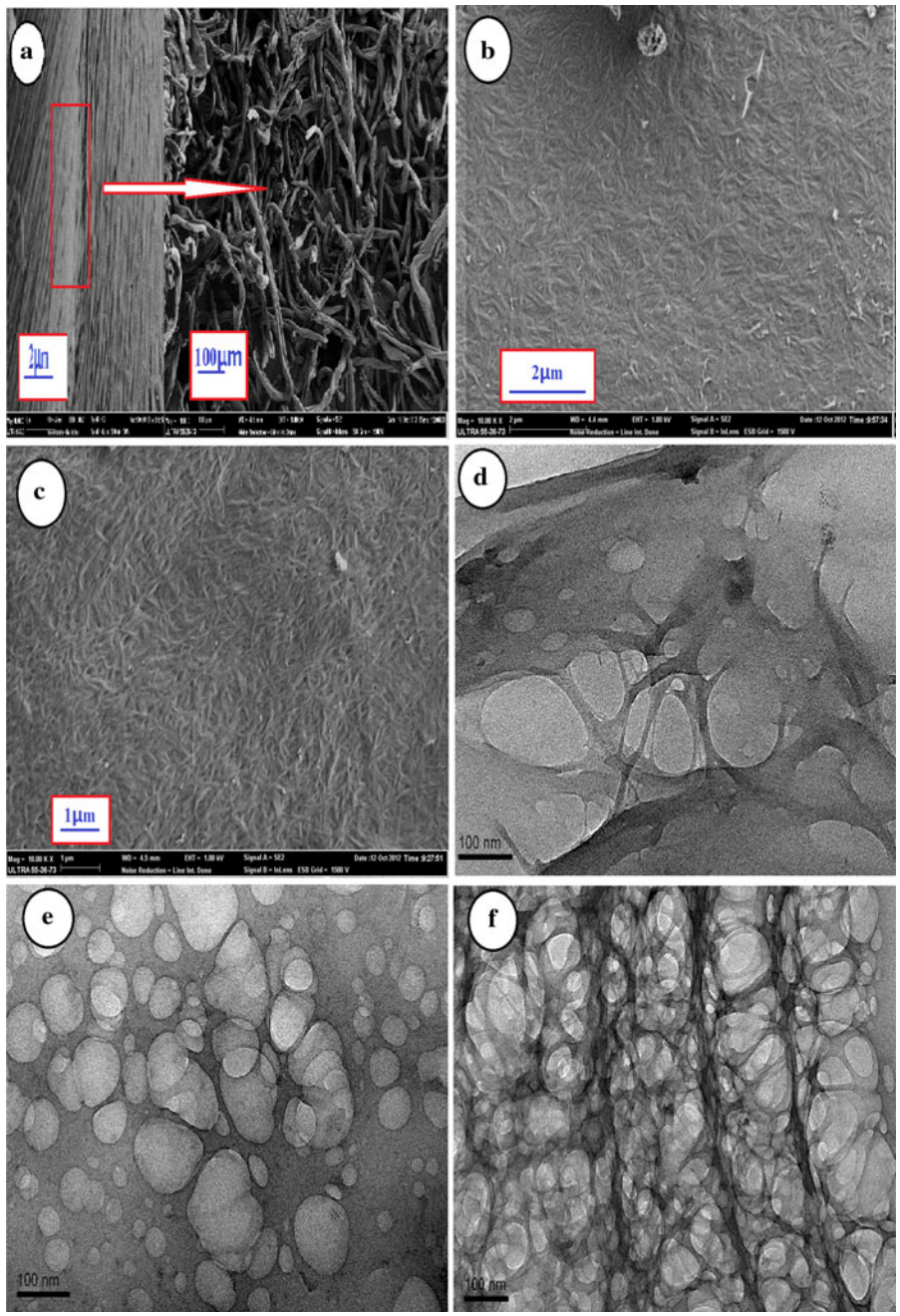

Fig. 2 SEM images of **a** raw MCC, **b** NCC-65 and **c** NCC-65-30; TEM images of **d** raw MCC, **e** NCC-65 and **f** NCC-65-30

shown in Fig. 3. For MCC sample (Fig. 3a), no particles had their sizes less than 40 μm, and the majority of MCC particles were in the range from 50 to 220 μm. For NCC samples (Fig. 3b), NCC-65 and NCC-65-30 exhibited a similar trend in PSD, whereas the latter showed a narrower distribution in particle size as a result of the assisted ultrasonic treatment. Moreover, based on the curves presented in Fig. 3, the average particle sizes of NCC-65-30 and NCC-65 were calculated as 368.60 and 373.70 nm, respectively, which was slightly higher than the recently reported value (Fan and Li 2012), where the average

particle size of NCC from cotton pulp by sulfuric acid hydrolysis was measured as 332.4 nm.

FT-IR spectra analysis

Figure 4 shows the FT-IR spectra of MCC, NCC-65, and NCC-65-30, respectively. As a whole, for MCC and NCC samples, a strong band appeared at approximately 3,340 cm^{-1}, which was related to the stretching vibration of O–H groups (Yang et al. 2011). The characteristic peak around 2,900 cm^{-1} was due to the symmetric C–H vibrations (Jahan et al. 2011; Zaman et al. 2012b). Similarly, an intense adsorption around 1,640 cm^{-1} originated from the absorbed water. Furthermore, the peaks at around 1,120, 1,030 and 665 cm^{-1} were attributed to the stretching vibration intermolecular ester bonding, stretching vibration of C–O (Sun et al. 2005) and C–OH (Cha et al. 2012; Wang et al. 2007) out-of-plane bending mode, respectively. More importantly, the intensity of most of the peaks of NCC-65 and NCC-65-30 was found to be significantly lower than that of MCC, such as the peaks at 3,340, 2,900, 1,370, 1,120, and 1,030 cm^{-1} (Fig. 4). The intensity of this absorption was considered to result from the oxidation of the cellulose during the acid hydrolysis reaction (Qua et al. 2011; Tamada 2003). Overall, although there was a significant decrease in the intensity of some peaks, NCC-65 and NCC-65-30 essentially showed the same spectra as the MCC. No obvious difference can be found in the FT-IR spectra between NCC-65 and NCC-65-30. All of the above results supported the conclusion that the molecular structures of cellulose remained unchanged in the presence of sulfuric acid hydrolysis process and ultrasonic treatment (Chen et al. 2011a).

Crystal structure by X-ray diffraction

XRDs of MCC, NCC-65 and NCC-65-30 are demonstrated in Fig. 5a–c, respectively. The NCC samples obtained in presence or absence of ultrasonic treatment, as well as the original MCC powder, exhibit the well-known peaks of 1–10, 110 and 200, which were in agreement with the characteristic diffraction peaks of cellulose Iβ (Savadekar and Mhaske 2012; Tonoli et al. 2012). This indicated that none of the chemical or ultrasonic treatments altered the main crystal structure of cellulose nanofibers, in accord with the FT-IR results. However, some slight differences in the diffraction patterns exist for the above samples. In contrast to MCC, the reduction of the intensities of the

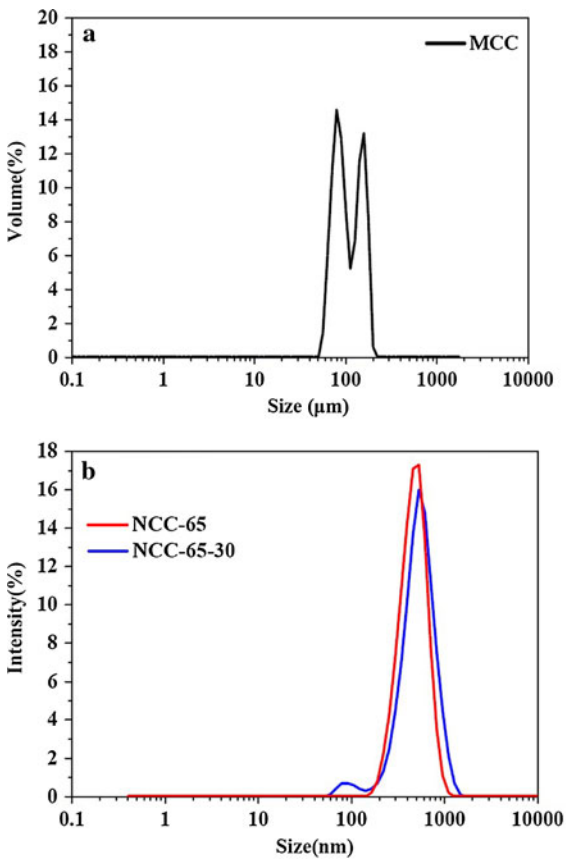

Fig. 3 Praticle size distribution of **a** raw MCC, **b** NCC-65 and NCC-65-30

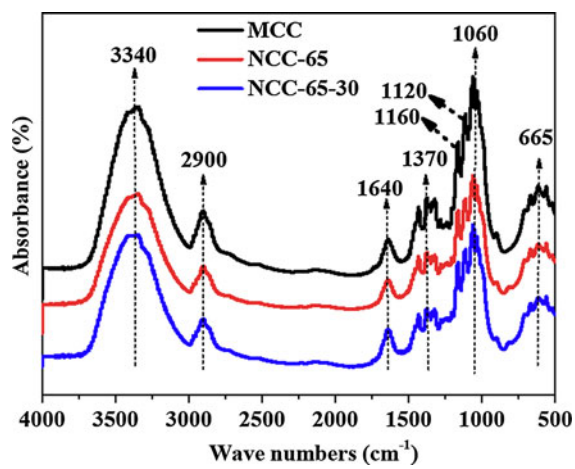

Fig. 4 FT-IR spectra of raw MCC, NCC-65 and NCC-65-30

(102) and (012) reflections as well as the peaks around (004) of NCC-65 was observed, likely due to preferred orientation (French 2014). In addition, the two small peaks of NCC-65-30 located at about 2-θ of 12° and 28° (marked 1 and 2 with dotted circle line in Fig. 5c) could result from the presence of a small amount of cellulose II.

The crystallinity of cellulose nanofibers is known as one of the most important factors determining their mechanical and thermal properties. There are various available methods for crystallinity measurement, such as XRD, solid state ^{13}C CP-MAS NMR, FT-IR spectroscopy and Raman spectroscopy (Terinte et al. 2011). The Segal CI was considered as a means of rapidly determining the relative crystallinity of various samples, based on the results of a powder diffractometer X-ray experiment (French 2014). Although the Segal CI has been used for more than 50 years, it has been questioned in recent years (Driemeier and Calligaris 2010; Park et al. 2010).

Recently, it was proposed that the crystallite size was of greater importance to describe the crystal structure of cellulose (Nishiyama et al. 2012). Interpreting diffraction patterns with atomistic molecular models is receiving increasing attention, since a model can provide the details of a structure that exhibits a calculated pattern similar to that from an XRD experiment. Here, the calculated diffraction patterns corresponding to the XRD patterns for MCC, NCC-65 and NCC-65-30 were achieved, and the corresponding numerical values of the Segal CI and crystallite size of all samples were calculated, both of which are presented in Fig. 5a–c, respectively. Notably, NCC-65-30 was found to possess a higher crystallinity in comparison with MCC and NCC-65, implying that low-ultrasonic treatment introduced to further facilitate the extraction of NCC exerted a positive impact on the NCC crystallinity. On the contrary, high-ultrasonic treatment generated a negative effect on the crystallinity of cellulose nanofibers, which had been well described in the recently reported literature (Li W et al. 2012). In their work, it was found that the crystallinity depended mainly on the ultrasonic time. After high-ultrasonic treatment (1,500 W) for 15 min, the crystallinity decreased from 82 % for raw MCC to 73 % for NCC. They attributed the significant decrease in crystallinity to the non-selective effect of ultrasonication, meaning

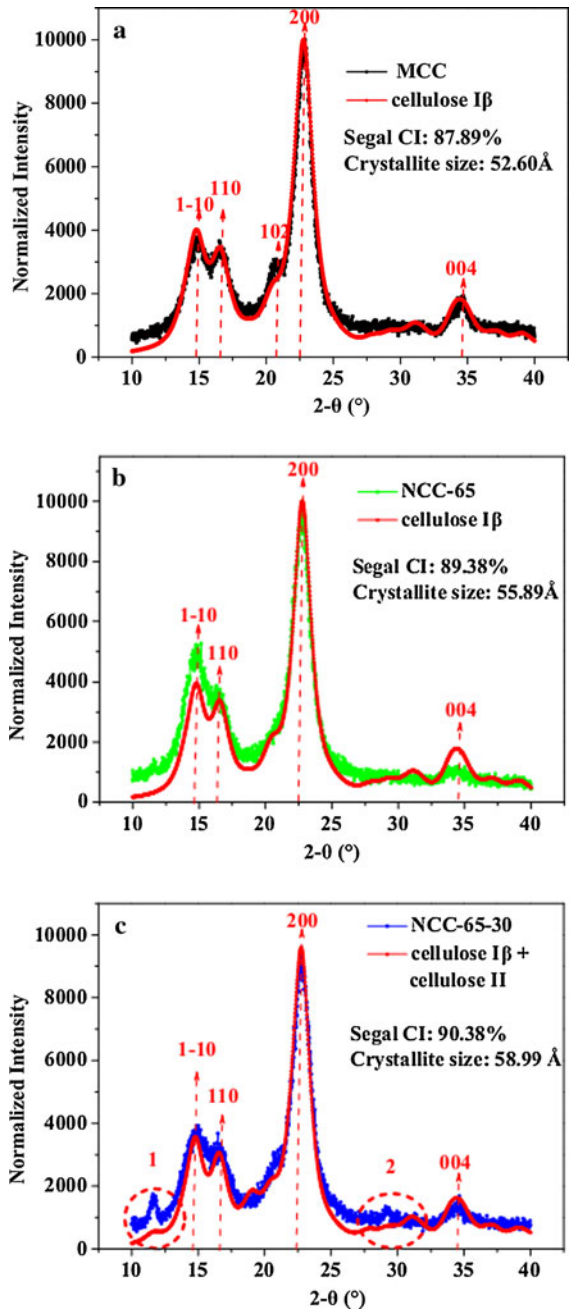

Fig. 5 **a** X-ray diffraction patterns for MCC and the calculated diffraction patterns for cellulose Iβ calculated for peak widths at half maximum of 1.7. **b** XRD patterns for NCC-65 and the calculated diffraction patterns for cellulose Iβ calculated for peak widths at half maximum of 1.6. **c** XRD patterns for NCC-65-30 and the calculated diffraction patterns for 90 % cellulose Iβ calculated for peak widths at half maximum of 1.5 and 10 % cellulose II calculated for peak widths at half maximum of 1.5

that it can remove both amorphous and crystalline cellulose. Therefore, it can be concluded that low-ultrasonic treatment showed more favorable effect on the NCC crystallinity than high-ultrasonic treatment. In addition, NCC-65-30 was also observed to exhibit the highest value in the calculated crystallite size among all the samples, which further confirmed the contribution of low-ultrasonic treatment to the crystal structure of nanocrystals.

Thermostability analysis

Figure 6a shows the thermal behaviors of raw MCC, NCC-65, and NCC-65-30. The initial small weight loss (around 5 %) at a low temperature (<100 °C) corresponded to the evaporation of absorbed water. For MCC, there was a slight weight loss up to 240 °C, and a drastic loss at 240–425 °C, followed by slow weight losses up to 780 °C. These results are similar to those reported in the previous publications (Ishida et al. 2004; Morán et al. 2008). For NCC-65, the vast majority of weight loss occurred in the range of 160–400 °C. For NCC-65-30, a significant weight loss started at around 180 °C and ended at 400 °C. Furthermore, based on the DTG curves in Fig. 6b, the thermal decomposition peaks of the maximum weight loss appeared at 290, 240, and 250 °C for MCC, NCC-65 and NCC-65-30, respectively. All of the above results indicated that the thermal stability of NCC samples was lower than that of MCC. It is widely accepted that the negative charged sulfonic groups introduced into the outer surface of the cellulose crystals resulted in the decrease in the thermal stability (de Morais Teixeira et al. 2010). In addition, the amounts of the char residues for MCC, NCC-65, and NCC-65-30 were 3.58, 7.38, and 8.93 %, respectively (see Fig. 6a). The increase in char residue for NCC samples might be attributed to the small size and increased number of free-end chains (Li W et al. 2012). Generally, NCC-65-30 and NCC-65 at TG or DTG curves were found to show an extremely similar tendency of changes, which further demonstrates that low-intensity ultrasonic treatment may facilitate the acid hydrolysis of cellulose under a fairly mild cavitation.

Rheological behavior of NCC suspensions

The properties of NCC-based composites produced by fluid phase processing are dependent on the NCC type, the dispersion microstructure, and the processing conditions (Urena-Benavides et al. 2011). One approach

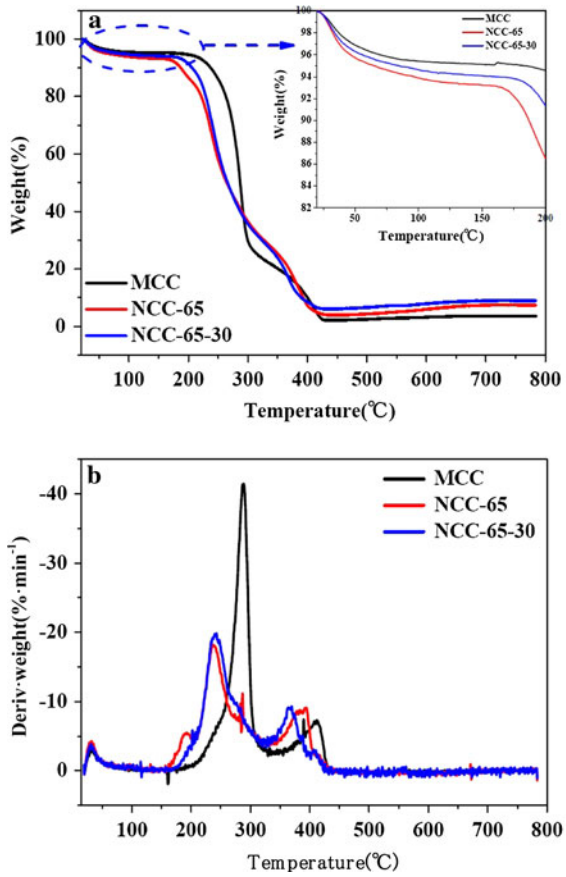

Fig. 6 **a** TG-curves and **b** DTG-curves of raw MCC, NCC-65 and NCC-65-30

to evaluate the dispersion microstructure and the processing properties of NCC suspensions would be to study the rheological behavior. According to previous studies (Chen et al. 2013; Liu et al. 2011; Urena-Benavides et al. 2011), the rheological behavior of NCC suspensions is strongly linked to the concentration, shear stress, and NCC production process. Therefore, the understanding of the rheological behavior of NCC suspensions from low-intensity ultrasonic-assisted sulfuric acid hydrolysis is of both scientific interest and practical relevance. NCC-65 and NCC-65-30 samples were dispersed into water to form stable aqueous suspensions with the same concentration of 0.77 %. The viscosity of the NCC-65 and NCC-65-30 suspensions as a function of shear rate from 0.1 to 100 s^{-1} is shown in Fig. 7. The shear-dependence of the viscosity profile showed that both suspensions exhibited a shear-thinning behavior, indicating that the apparent viscosity decreased with the increased shear rate. Moreover, it was found that the NCC-65-30

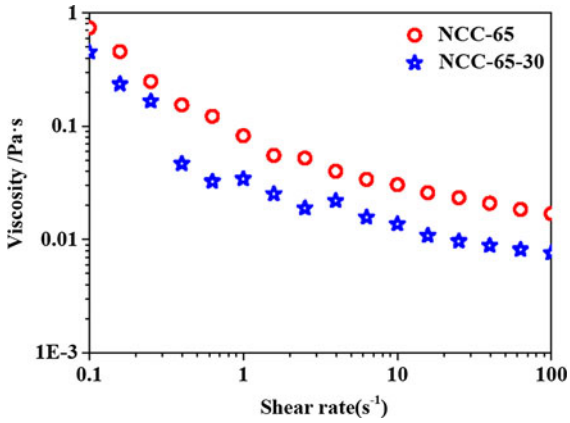

Fig. 7 Viscosity as a function of shear rate for NCC-65 and NCC-65-30 suspensions

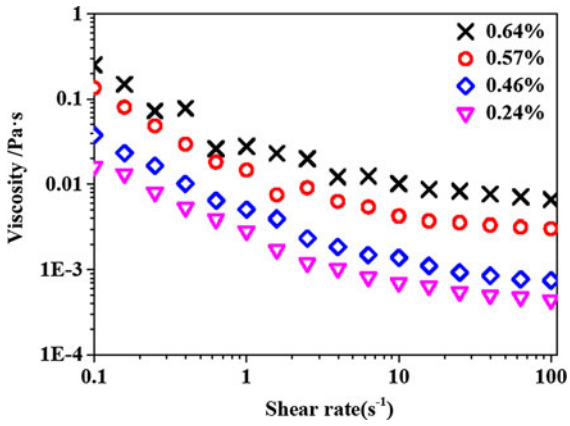

Fig. 8 Viscosity as a function of shear rate for NCC-65-30 suspensions with different concentrations

suspensions displayed a lower viscosity than NCC-65 suspensions at the same shear rate, which may be explained by the presence of the ultrasonic treatment, resulting in the decrease of the degree of polymerization (Hamada and Bousfield 2010).

In addition, a series of NCC-65-30 suspensions were made at the concentrations of 0.24, 0.46, 0.57 and 0.64 %, and their viscosity-shear rate curves are shown in Fig. 8. As expected, the shear-thinning behavior can also be observed over the entire range of shear rates for all the NCC suspensions. Overall, it can be found that the viscosity of NCC suspension was highly dependent on the concentration, showing a steady increase with the concentration variations ranging from 0.24, 0.46, 0.57 to 0.64 %, which is similar to the results reported by Liu et al. (2011).

Conclusion

The NCC yield is a key factor determining the economics of acid hydrolysis. In the present work, a low-intensity ultrasonication concept was employed to improve the yield of NCC based on sulfuric acid hydrolysis. The results showed that the NCC yield increased from 33.0 % from the conventional hydrolysis method to 40.4 % from the ultrasonic-assisted process, based on a 65 wt% sulfuric acid concentration and 30 min low-intensity ultrasonication. TEM, and SEM results showed the rod shaped NCC with diameters of 10–20 nm. XRD indicated that low-ultrasonic treatment introduced to further facilitate the extraction of NCC led to the increased Segal CI and crystallite size of NCC. Ultrasonic treatment was found to exert a limited effect on the thermal behavior of NCC. When dispersed in water, the NCC suspensions from the ultrasonic-assisted process gave a lower viscosity at the same shear rate.

Acknowledgments This work was financially supported by the National Natural Science Foundation of China (Grant No. 31100442), the Science and Technology Program of Hangzhou City of China (Grant No. 20120433B63), the Science and Technology Program of Zhejiang Environmental Protection Bureau of China (Grant No. 2012B008), Zhejiang Provincial Top Key Academic Discipline of Chemical Engineering and Technology and 521 Talent Cultivation Program of Zhejiang Sci-Tech University (Grant No. 11110132521310).

References

Ahmadi F, McLoughlin IV, Chauhan S, Ter-Haar G (2012) Bio-effects and safety of low-intensity, low-frequency ultrasonic exposure. Prog Biophys Mol Biol 108(3):119–138

Bai W, Holbery J, Li K (2009) A technique for production of nanocrystalline cellulose with a narrow size distribution. Cellulose 16(3):455–465

Beck-Candanedo S, Roman M, Gray DG (2005) Effect of reaction conditions on the properties and behavior of wood cellulose nanocrystal suspensions. Biomacromolecules 6(2):1048–1054

Bondeson D, Mathew A, Oksman K (2006) Optimization of the isolation of nanocrystals from microcrystalline cellulose by acid hydrolysis. Cellulose 13(2):171–180

Brinchi L, Cotana F, Fortunati E, Kenny JM (2013) Production of nanocrystalline cellulose from lignocellulosic biomass: technology and applications. Carbohydr Polym 94(1):154–169

Cha R, He Z, Ni Y (2012) Preparation and characterization of thermal/pH-sensitive hydrogel from carboxylated nanocrystalline cellulose. Carbohydr Polym 88(2):713–718

Chen W, Yu H, Liu Y (2011a) Preparation of millimeter-long cellulose I nanofibers with diameters of 30–80 nm from bamboo fibers. Carbohydr Polym 86(2):453–461

Chen W, Yu H, Liu Y, Chen P, Zhang M, Hai Y (2011b) Individualization of cellulose nanofibers from wood using high-intensity ultrasonication combined with chemical pretreatments. Carbohydr Polym 83(4):1804–1811

Chen W, Yu H, Liu Y, Hai Y, Zhang M, Chen P (2011c) Isolation and characterization of cellulose nanofibers from four plant cellulose fibers using a chemical-ultrasonic process. Cellulose 18(2):433–442

Chen P, Yu H, Liu Y, Chen W, Wang X, Ouyang M (2013) Concentration effects on the isolation and dynamic rheological behavior of cellulose nanofibers via ultrasonic processing. Cellulose 20(1):149–157

Cintas P, Luche J (1999) Green chemistry. The sonochemical approach. Green Chem 1(3):115–125

de Campos A, Correa AC, Cannella D, de Morais Teixeira E, Marconcini JM, Dufresne A, Mattoso LH, Cassland P, Sanadi AR (2013) Obtaining nanofibers from curauá and sugarcane bagasse fibers using enzymatic hydrolysis followed by sonication. Cellulose 20(3):1491–1500

de Morais Teixeira E, Corrêa AC, Manzoli A, de Lima LeiteF, de Oliveira CR, Mattoso LHC (2010) Cellulose nanofibers from white and naturally colored cotton fibers. Cellulose 17(3):595–606

Deepa B, Abraham E, Cherian BM, Bismarck A, Blaker JJ, Pothan LA, Leao AL, de Souza SF, Kottaisamy M (2011) Structure, morphology and thermal characteristics of banana nano fibers obtained by steam explosion. Bioresour Technol 102(2):1988–1997

Driemeier C, Calligaris GA (2010) Theoretical and experimental developments for accurate determination of crystallinity of cellulose I materials. J Appl Crystallogr 44(1):184–192

Elazzouzi-Hafraoui S, Nishiyama Y, Putaux J, Heux L, Dubreuil F, Rochas C (2007) The shape and size distribution of crystalline nanoparticles prepared by acid hydrolysis of native cellulose. Biomacromolecules 9(1):57–65

Eronen P, Österberg M, Heikkinen S, Tenkanen M, Laine J (2011) Interactions of structurally different hemicelluloses with nanofibrillar cellulose. Carbohydr Polym 86(3):1281–1290

Fan J, Li Y (2012) Maximizing the yield of nanocrystalline cellulose from cotton pulp fiber. Carbohydr Polym 88(4):1184–1188

Fatehi P, Liu X, Ni Y, Xiao H (2010) Interaction of cationic modified poly vinyl alcohol with high yield pulp. Cellulose 17(5):1021–1031

Filson PB, Dawson-Andoh BE (2009) Sono-chemical preparation of cellulose nanocrystals from lignocellulose derived materials. Bioresour Technol 100(7):2259–2264

French AD (2014) Idealized powder diffraction patterns for cellulose polymorphs. Cellulose. doi:10.1007/s10570-013-0030-4

French AD, Santiago Cintrón M (2013) Cellulose polymorphy, crystallite size, and the Segal Crystallinity Index. Cellulose 20(1):583–588

Hamad WY, Hu TQ (2010) Structure–process–yield interrelations in nanocrystalline cellulose extraction. Can J Chem Eng 88(3):392–402

Hamada H, Bousfield DW (2010) Nano-fibrillated cellulose as a coating agent to improve print quality of synthetic fiber sheets. In: TAPPI 11th advanced coating fundamentals symposium, Munich, TAPPI, Atlanta, GA, pp 7–16

Hashaikeh R, Abushammala H (2011) Acid mediated networked cellulose: preparation and characterization. Carbohydr Polym 83(3):1088–1094

Henriksson M, Henriksson G, Berglund LA, Lindström T (2007) An environmentally friendly method for enzyme-assisted preparation of microfibrillated cellulose (MFC) nanofibers. Eur Poly J 43(8):3434–3441

Ishida O, Kim D, Kuga S, Nishiyama Y, Brown RM (2004) Microfibrillar carbon from native cellulose. Cellulose 11(3–4):475–480

Jahan MS, Saeed A, He Z, Ni Y (2011) Jute as raw material for the preparation of microcrystalline cellulose. Cellulose 18(2):451–459

Johar N, Ahmad I, Dufresne A (2012) Extraction, preparation and characterization of cellulose fibres and nanocrystals from rice husk. Ind Crop Prod 37(1):93–99

Klemm D, Schumann D, Udhardt U, Marsch S (2001) Bacterial synthesized cellulose—artificial blood vessels for microsurgery. Prog Polym Sci 26(9):1561–1603

Lam E, Male KB, Chong JH, Leung ACW, Luong JHT (2012) Applications of functionalized and nanoparticle-modified nanocrystalline cellulose. Trends Biotechnol 30(5):283–290

Langan P, Nishiyama Y, Chanzy H (2001) X-ray structure of mercerized cellulose II at 1 Å resolution. Biomacromolecules 2(2):410–416. doi:10.1021/bm005612q

Li J, Wei X, Wang Q, Chen J, Chang G, Kong L, Su J, Liu Y (2012) Homogeneous isolation of nanocellulose from sugarcane bagasse by high pressure homogenization. Carbohydr Polym 90(4):1609–1613

Li W, Yue J, Liu S (2012) Preparation of nanocrystalline cellulose via ultrasound and its reinforcement capability for poly(vinyl alcohol) composites. Ultrason Sonochem 19(3):479–485

Liu D, Chen X, Yue Y, Chen M, Wu Q (2011) Structure and rheology of nanocrystalline cellulose. Carbohydr Polym 84(1):316–322

Liu C, Xiao B, Dauta A, Peng G, Liu S, Hu Z (2009) Effect of low power ultrasonic radiation on anaerobic biodegradability of sewage sludge. Bioresour Technol 100(24):6217–6222

Lu P, Hsieh Y (2010) Preparation and properties of cellulose nanocrystals: rods, spheres, and network. Carbohydr Polym 82(2):329–336

Lu H, Gui Y, Zheng L, Liu X (2013) Morphological, crystalline, thermal and physicochemical properties of cellulose nanocrystals obtained from sweet potato residue. Food Res Int 50(1):121–128

Morais JPS, Rosa MDF, Nasciment LD, Nascimento DMD, Alexandre LC (2012) Extraction and characterization of nanocellulose structures from raw cotton linter. Carbohydr Polym 91(1):229–235

Morán JI, Alvarez VA, Cyras VP, Vázquez A (2008) Extraction of cellulose and preparation of nanocellulose from sisal fibers. Cellulose 15(1):149–159

Nishiyama Y, Langan P, Chanzy H (2002) Crystal structure and hydrogen-bonding system in cellulose Iβ from synchrotron X-ray and neutron fiber diffraction. J Am Chem Soc 124(31):9074–9082

Nishiyama Y, Johnson GP, French AD (2012) Diffraction from nonperiodic models of cellulose crystals. Cellulose 19(2):319–336

Okahisa Y, Abe K, Nogi M, Nakagaito AN, Nakatani T, Yano H (2011) Effects of delignification in the production of plant-based cellulose nanofibers for optically transparent nanocomposites. Compos Sci Technol 71(10):1342–1347

Park S, Baker JO, Himmel ME, Parilla PA, Johnson DK (2010) Cellulose crystallinity index: measurement techniques and their impact on interpreting cellulase performance. Biotechnol Biofuels 3:1–10

Pirani S, Hashaikeh R (2012) Nanocrystalline cellulose extraction process and utilization of the byproduct for biofuels production. Carbohydr Polym 93(1):357–363

Pourbafarani S, Mozaffari M, Amighian J (2013) Investigation of phase formation and magnetic properties of Mn ferrite nanoparticles prepared via low-power ultrasonic assisted co-precipitation method. J Supercond Nov Magn 26(3):675–678

Qian L, Guan Y, Ziaee Z, He B, Zheng A, Xiao H (2009) Rendering cellulose fibers antimicrobial using cationic β-cyclodextrin-based polymers included with antibiotics. Cellulose 16(2):309–317

Qua EH, Hornsby PR, Sharma H, Lyons G (2011) Preparation and characterisation of cellulose nanofibres. J Mater Sci 46(18):6029–6045

Roman M, Winter WT (2004) Effect of sulfate groups from sulfuric acid hydrolysis on the thermal degradation behavior of bacterial cellulose. Biomacromolecules 5(5):1671–1677

Satyamurthy P, Jain P, Balasubramanya RH, Vigneshwaran N (2011) Preparation and characterization of cellulose nanowhiskers from cotton fibres by controlled microbial hydrolysis. Carbohydr Polym 83(1):122–129

Savadekar NR, Mhaske ST (2012) Synthesis of nano cellulose fibers and effect on thermoplastics starch based films. Carbohydr Polym 89(1):146–151

Scherrer P (1918) Bestimmung der Grösse und der inneren Struktur von Kolloidteilchen mittels Röntgenstrahlen. Nachr Ges Wiss Göttingen 26:98–100

Sun XF, Xu F, Sun RC, Fowler P, Baird MS (2005) Characteristics of degraded cellulose obtained from steam-exploded wheat straw. Carbohydr Res 340(1):97–106

Tamada Y (2003) Sulfation of silk fibroin by sulfuric acid and anticoagulant activity. J App Poly Sci 87(14):2377–2382

Tang L, Huang B, Lu Q, Wang S, Ou W, Lin W, Chen X (2012) Ultrasonication-assisted manufacture of cellulose nanocrystals esterified with acetic acid. Bioresour Technol 127:100–105

Terinte N, Ibbett R, Schuster KC (2011) Overview on native cellulose and microcrystalline cellulose I structure studied by X-ray diffraction (WAXD): comparison between measurement techniques. Lenzingr Ber 89:118–131

Tischer PCF, Sierakowski MR, Westfahl H Jr, Tischer CA (2010) Nanostructural reorganization of bacterial cellulose by ultrasonic treatment. Biomacromolecules 11(5):1217–1224

Tonoli GHD, Teixeira EM, Corrêa AC, Marconcini JM, Caixeta LA, Pereira-da-Silva MA, Mattoso LHC (2012) Cellulose micro/nanofibres from *Eucalyptus* kraft pulp: preparation and properties. Carbohydr Polym 89(1):80–88

Torvinen K, Sievänen J, Hjelt T, Hellén E (2012) Smooth and flexible filler-nanocellulose composite structure for printed electronics applications. Cellulose 19(3):821–829

Urena-Benavides EE, Ao G, Davis VA, Kitchens CL (2011) Rheology and phase behavior of lyotropic cellulose nanocrystal suspensions. Macromolecules 44(22):8990–8998

Wang N, Ding E, Cheng R (2007) Thermal degradation behaviors of spherical cellulose nanocrystals with sulfate groups. Polymer 48(12):3486–3493

Wang N, Ding E, Cheng R (2008) Preparation and liquid crystalline properties of spherical cellulose nanocrystals. Langmuir 24(1):5–8

Yang Q, Pan X, Huang F, Li K (2011) Synthesis and characterization of cellulose fibers grafted with hyperbranched poly (3-methyl-3-oxetanemethanol). Cellulose 18(6):1611–1621

Zaman M, Liu H, Xiao H, Chibante F, Ni Y (2012a) Hydrophilic modification of polyester fabric by applying nanocrystalline cellulose containing surface finish. Carbohydr Polym 91(2):560–567

Zaman M, Xiao H, Chibante F, Ni Y (2012b) Synthesis and characterization of cationically modified nanocrystalline cellulose. Carbohydr Polym 89(1):163–170